

# Experimental and Numerical Investigation of Different Types of Jacketing Effect on Retrofitting RC Short Columns Using ECC Concrete

Behrooz Dadmand<sup>1</sup>, Masoud Pourbaba<sup>2\*</sup>, Ramin Riahi<sup>3</sup>

<sup>1</sup> Department of Civil Engineering, Razi University, 6714414971 Kermanshah, Iran

<sup>2</sup> Department of Civil and Environmental Engineering, Research Scholar, University of Houston, 4800 Calhoun Rd, TX 77004 Houston, Texas, USA

<sup>3</sup> Department of Civil Engineering, K. N. Toosi University of Technology, 470 Mirdamad Ave. West, 19697 Tehran, Iran

\* Corresponding author, e-mail: [mpourbab@central.uh.edu](mailto:mpourbab@central.uh.edu)

Received: 21 August 2021, Accepted: 22 February 2022, Published online: 09 March 2022

## Abstract

Given the deterioration of civil infrastructure throughout the world, developing more efficient repair and strengthening is essential. Jacketing is one of the most common methods for retrofitting reinforced concrete (RC) columns. Notably, using engineered cementitious composite (ECC) within the jacketing area increases the bearing capacity and significantly enhances the ductility of the columns. The recent development of ECC concrete with suitable compressive strength and higher ductility of about 5 % can significantly enhance the performance of reinforced concrete structures. The behavior of retrofitted RC columns depends heavily on the cohesion between the jacket and the original column as well as the mechanical properties of the jacketing materials. This study investigates jacketed square and circular RC columns using ECC and conventional/normal concrete (NC) using different casing techniques to retrofit RC columns, namely galvanized mesh, U and L-shape joints, removing the cover, core drilling, and integrated models. All specimens were subjected to a compression test. The results indicate that in both square and circular specimens, the use of ECC as a super ductile material and vertical U-shaped elements to connect the longitudinal rebars of the casing and the core leads to much higher ductility and bearing capacity than in NC specimens. These elements also showed suitable ductility because of using ECC as a super ductile material. In order to optimize these methods, finite element analysis (FEA) was conducted using Abaqus software to verify experimental models, as well as a parametric study to achieve an optimum design of the jacketing.

## Keywords

repair, jacketing techniques, retrofitting, RC short columns, engineered cementitious composite (ECC)

## 1 Introduction

It is well acknowledged that many members of older structures cannot meet the load-bearing capacity of the original design due to concrete cracking, rust corrosion, or other factors and damage [1]. Rehabilitation of reinforced concrete (RC) structures is an alternative to demolition and rebuilding, saving operational costs and time. Among all RC structure reinstatement methods, several attempts have been made to numerically and experimentally investigate the jacketing strengthening technique as a feasible solution. A considerable amount of literature has focused on different methods of RC structure reinstatement, such as concrete jacketing, steel jacketing, and fiber-reinforced polymer (FRP) jacketing [2]. In general, one can say that jacketing effectively strengthens RC structures and

enhances compressive strength, ductility, Deformation capacity, and toughness [3]. This technique is mainly used for building columns, but this method has also been used in Japan to strengthen the foundations of a number of stairs. More confinement is created by twisting or tighter reinforcement [4]. Concrete pods can be used to reinforce beams as well as columns [5].

Most concrete structures are repaired or reinforced with concrete jacketing to address structural safety concerns. Also, when corrosion occurs in the steel reinforcement of the building, structural repairs seem necessary as a practical solution. In experiments, Ersoy et al. [3] and Lehman et al. [6] proved the success of using concrete jacketing to repair RC columns. The most important aspects of the

study are the effect of preloading, prevention of shear failure, the effect of repair by concrete jacketing, the effect on ductility, and the effect of the joint surface between the core and casing. Lehman et al. [6] used a concrete jacket to repair severely damaged columns. Their results indicated that the RC jacketed column illustrated more stiffness and strength than the initial column. Vadoros and Dritsos [7] investigated the effect of preloading on the behavior of the retrofitted column.

The RC columns were subjected to axial and lateral loads. The results showed that preloading increases resistance and deformation capacity [7]. Bett et al. [8] observed flexural cracks in columns reinforced with concrete jackets at a relative lateral displacement level of less than one percent. Studies by Thermou et al. [9] showed that concrete jacketing increases the stiffness and strength of a structural member. The change in the deformable capacity of the member depends on factors such as the aspect ratio of the jacketed member and the limiting factors of deformable capacity in the initial conditions of the structure. Ong et al. [10] have studied the RC square columns by the concrete jacket method. The results indicated that the concrete jacket increases the axial bearing capacity; the strain increases at the point of maximum axial force, and the ductility increases after that point. Vadoros and Dritsos [11] investigated the effect of different bonding methods on columns enclosed by RC jackets.

The results showed that the contact between casing and core is highly significant, affecting ductility and energy dissipation capacity [11]. The confinement created by the transverse reinforcement increases the concrete strength, strain at maximum stress, and ductility [12]. Models used to estimate the strength of enclosed concrete in steel can also be generalized to determine the strength of enclosed concrete with other materials. The enclosed concrete models have been evaluated by many researchers [12–16]. The most common model used to estimate the strength of enclosed concrete is the model proposed by Mander et al. [14, 15]. This model is presented for concrete enclosed by transverse steel reinforcements. The energy balance method was used to predict the longitudinal compressive strain of the concrete related to the first failure of the transverse reinforcement. The strain energy capacity of the transverse reinforcement is assumed to be equal to the strain energy stored in the concrete due to the confinement. This theoretical model is based on a laboratory study performed on 40 axial compression tests. These experiments included circular, square, and rectangular reinforced concrete columns subjected to rapid and low-speed axial loading.

Nowadays, with advancements in concrete technology, engineers have a broader trend toward using concrete with high tensile properties. Therefore, some researchers have developed various fibers such as steel, carbon, glass, synthetics, and even hybrids that combine different fiber types [17–18]. Various fibers, even in small dosage, have been successfully used in improving tensile strain capacity, compressive strength, and some other mechanical properties of these kinds of concrete, such as fiber reinforced concrete (FRC), ultra-high-performance fiber-reinforced concrete (UHPFRC) [19–21]. In general, these kinds of concrete do not contain any coarse aggregates in front of conventional concrete [22–24]. The demands for higher ductility caused to development of the engineered cementitious composite (ECC) at the University of Michigan by Li [25–27] and Li et al. [28] with ideal ductility and suitable tensile strength. Concrete jacketing is still considered one of the main reinforcement methods, mainly when the other rehabilitation methods are impossible; this is because the positive effect of creating a concrete jacket around a reinforced concrete column has been proven both in increasing the bearing capacity in increasing its ductility. The behavior of jacketed columns with concrete is directly related to the degree of cohesion of the jacket and the initial column and the material property of concrete used in the jacketing area. Because if a good connection is established at the joint surface of the jacket and the primary column, the behavior of the reinforced column will be closer to the behavior of the integrated specimen. Krishnaraja and Kandasamy [29] have evaluated the effect of ECC layers on concrete beams, which is similar to the purpose of this research. They have concluded that compared with the conventional concrete beam, the ECC layer presence not only leads to significant enhancement in the cracking load, yielding load and ultimate load but also increases the load-bearing capacity, deflection, energy absorption, and ductility due to strain hardening of ECC layer in the concrete beam.

Additionally, using ECC as the jacketing part regarding its exceptional properties, such as high tensile strain capacity (5%) and fine crack widths, can improve the retrofitting performance. Therefore, in this research, experimental and numerical investigation of the effect of different types of jacketing using ECC concrete on retrofitting RC short columns have been studied.

## 2 Experimental program

The main focus of the experiments performed in this research is to investigate the effect of using ECC concrete as the jacketing material instead of conventional/normal

concrete (NC) and how to increase the concrete continuity of the core and casing. The typical mixed developed by Li [27] was used For ECC casting .

Table 1 provides the typical ECC mix proportions with poly-vinyl-alcohol (PVA) fiber 12 mm in length and 39 μm in diameter (with a tensile strength of 1600 MPa, and density of 1300 kg/m<sup>3</sup>). Other Constituents of the mix are as follows:

Portland cement type II (ASTM C150) [30], fly ash type F ASTM C618-19 [31], fine sand with a maximum diameter of 1.12 mm passed through sieve #16 and Type F water-reducing high-range polycarboxylate-based superplasticizer (ASTM C494) [32]. The superplasticizer used was AURAMIX 4450 (FOSROC), a polycarboxylic ether-based superplasticizer.

A suitable mix design was used in this experimental research to obtain high composite ductility, which has been used successfully in the previous works by authors [20–21].

As a former experience by authors [19], first, fly ash was mixed with all the sand for approximately 3 minutes. Then, cement was added and dry mixed for at least 4 minutes. Then, water and superplasticizer were added gradually and mixing continued for an additional 4 minutes to improve flowability and obtain a suitable paste. PVA fiber was added by 2.0% of the volume to improve the mechanical properties of ECC concrete, especially in terms of ductility and tensile capacity (Fig. 1).

After finishing the mixing process, ECC was poured into the jacketing part of cylindrical and cube molds. After 24 hours, the specimens were removed and transferred to the water tank under lab temperature until the testing day. Cubes of 100 × 100 × 100 mm, cylinders of 100 × 200 mm,

**Table 1** ECC Mix Proportions by weight [27]

Cement	Fly Ash	Sand	Water	Superplasticizer	Fiber (Vol%)
1.0	1.20	0.80	0.56	0.012	0.02

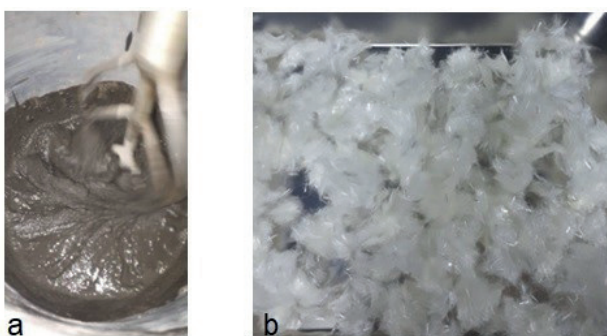


**Fig. 1** Mix design for experimental test, a) ECC mixing process and b) Close-up view of PVA fiber

and dog-bone specimens, according to Fig. 2, were also made to determine the compressive strength and direct tensile strength of ECC.

The specimens were made in a square and circular section in this research. In general, ten types of connections of specimens have been considered as follows:

1. Primary specimen with NC (unjacketed specimen as control sample); O-Type
2. Simple jacketing using NC; S-Type
3. Simple jacketing using ECC; G-Type
4. Use of L-shaped elements on the contact surface of the core and casing using ECC; L-Type
5. Use of galvanized mesh on the contact surface using ECC; W-Type
6. Using U-shaped curved elements to connect the longitudinal rebars using ECC; B-Type
7. Use of curved U-shaped elements horizontally on the contact surface using ECC; U-Type
8. Removing the concrete cover of the primary column using ECC; C-Type
9. Creating surface holes on the primary column using ECC; H-Type
10. Integrated sample with NC (simultaneous concreting of primary column and casing); M-Type

In this study, 24 specimens were made and subjected to compression testing until complete failure. Specimens have equal dimensions, longitudinal and transverse reinforcement. Twelve specimens had a circular cross-section, and the other 12 remaining specimens had a square cross-section. From each series of 12, 3 specimens were reinforced as control specimens (without making concrete jackets), eight specimens were retrofitted, and an integrated sample using NC is also provided for comparative purposes. The longitudinal and transverse reinforcements used in the jackets were the same as the reinforcements used in the core. Also, the used mixing design of NC was the same, and only in specimens with ECC concrete, the materials of the casing and the initial column were different. Table 2 lists the names of all the specimens and the number of each. The dimensions of the samples before and

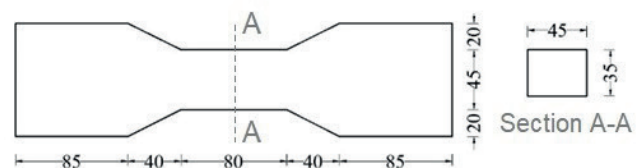


**Fig. 2** Dimensions of the dog-bone specimen for direct tension test (unit: mm) [22]

**Table 2** Studied specimens

Jacketing Type	Concrete Type	Name		Number
		Square	Circular	
No Jacketing	NC	S-O-1	C-O-1	6
		S-O-2	C-O-2	
		S-O-3	C-O-3	
Simple jacketing	NC	S-S	C-S	2
Integrated	NC	S-M	C-M	2
Simple jacketing	ECC	S-G	C-G	2
L-Shape elements	ECC	S-L	C-L	2
Galvanized Mesh	ECC	S-W	C-W	2
Vertical U-Shape element	ECC	S-B	C-B	2
Removing concrete Cover	ECC	S-C	C-C	2
U-Shape elements	ECC	S-U	C-U	2
Hole on surface	ECC	S-H	C-H	2

after jacketing were  $80 \times 80 \times 400$  mm ( $A = 64 \times 10^2$  mm<sup>2</sup>) and  $120 \times 120 \times 400$  mm ( $A = 144 \times 10^2$  mm<sup>2</sup>) in square columns, respectively, and  $90 \times 400$  mm ( $A = 63.6 \times 10^2$  mm<sup>2</sup>) and  $135 \times 400$  mm ( $A = 143 \times 10^2$  mm<sup>2</sup>) in circular columns, respectively, where A is the cross-sectional area. It is noteworthy that for better comparison the cross-sectional areas of the specimens are almost the same. The typical mixing design, including Portland cement, fine aggregate (maximum size of 20 mm), and water (with  $w/c = 0.45$ ), were used to make the NC for use in some of the specimens of this study.

**2.1 Concrete testing**

Cylindrical and cube samples with dimensions of  $150 \times 300$  mm and  $100 \times 100 \times 100$  mm were prepared for NC and ECC concrete, respectively. Additionally, dog-bone shape samples were taken from ECC concrete for the direct tensile strength tests. All tests were repeated three times to obtain the experiments' exact mechanical properties (Fig. 3). The average 28-day NC and ECC concrete compressive strengths were measured as 17 and 40 MPa, respectively. The tensile stress-strain curve of ECC concrete is illustrated in Fig. 4 as well. The ultimate tensile strength of ECC obtained from the dog-bone test was 7 MPa, as shown in Fig. 4.

**2.2 Steel rebars**

The steel rebars in the test specimens are as follows:

- 5 mm diameter screw to make L and U-shaped elements
- S400 class steel rebar as a longitudinal reinforcement of the primary column and casing with an 8 mm diameter

- A simple wire with a diameter of 2.5 mm as a transverse reinforcement of the primary column and casing.

In order to obtain steel rebar characteristics, several steel rebars were selected before making columns for the tensile strength test. The stress-strain curve obtained from the test showed that the rebar yield and ultimate strengths are 430 MPa and 660 MPa, respectively (see Table 3).

**2.3 Concreting the primary columns**

After preparing the concrete mixture, concreting is done in 5 layers. Jacket reinforcement is made the same way as in the construction of primary column reinforcement (see Fig. 5).

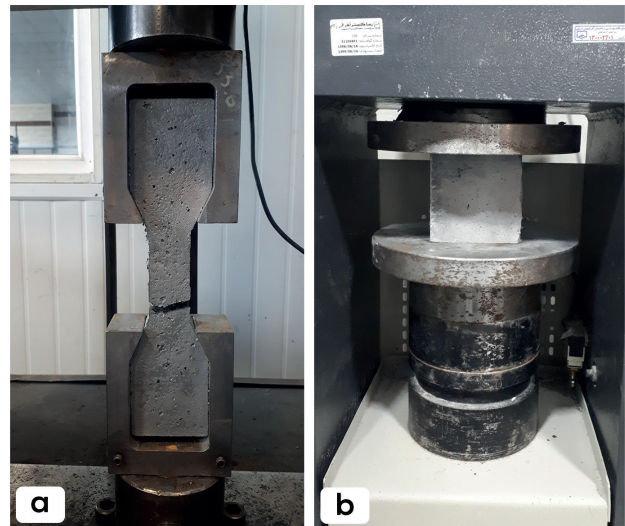


**Fig. 3** a) ECC dog-bone tension test, b) compressive strength test

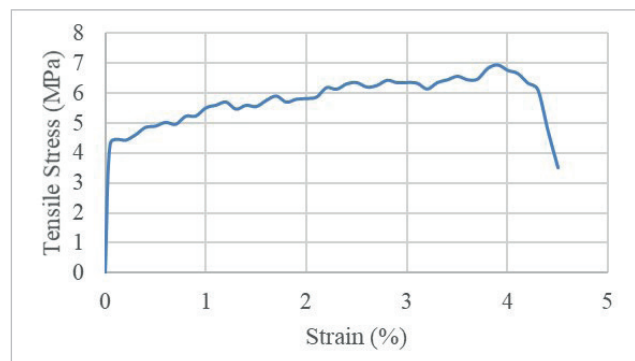


**Fig. 4** Tensile -strain curve for ECC specimen

**Table 3** Mechanical properties of steels according to tensile tests

	Diameter (mm)	Yield Stress (MPa)	Ultimate Stress (MPa)
Longitudinal rebar	8	430	660
Transverse rebar	2.5	240	405
Screw	5	430	550

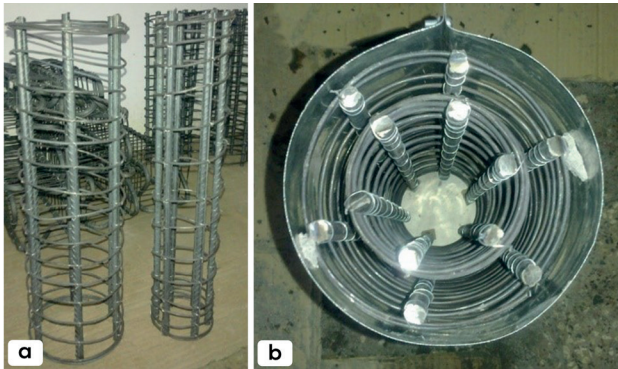


Fig. 5 a) Reinforcement, b) Placement of reinforcement in formwork

#### 2.4 Connection elements

Joints are considered to investigate the increased bonding of the concrete core with the casing and make closer the behavior of jacketed columns to the behavior of integrated ones. The connection elements considered in this research are L-shaped, U-shaped, and galvanized mesh (see Fig. 6).

#### 2.5 Experimental tests

Uniaxial compression loading tests were carried out on specimens after 28 days of casting. All specimens were tested using a testing machine with a capacity of 2000 KN. One millimeter/minute was used to load the specimens. The specimens are carefully placed in the machine's loading jaw center before commencing the tests (Fig. 7). All retrofitted specimens were loaded until displacement of about 50 mm, after which the test was stopped.

### 3 Test results and discussion

#### 3.1 Compressive strength

Table 4 summarizes test results for all square and circular specimens. The table also shows the maximum strength, the maximum force of specimens after retrofitting to a maximum force of specimens before retrofitting, primary specimens (O), and energy absorption of all specimens. The percentage of increase in the strength of the primary specimen due to the jacketing has been compared.

#### 3.2 Fracture modes

Since different kinds of concrete (NC and ECC) and different jacketing methods have been used, the degree of damage, ductility, and ultimate strength differ in the same displacement created in the specimens. Damage in jacketed specimens initiates with the formation of cracks in the concrete cover of the casing, which often occur longitudinally. Cracks and scaling of the concrete cover occur almost simultaneously. After peeling off the outer cover of



Fig. 6 Connecting elements and different specimens before concreting the casing



Fig. 7 Test setup for compressive experiments on short RC columns

the sample, buckling of longitudinal rebars occurs at the moment of reaching the final strength of the specimen. The next step is the failure of the transverse reinforcements, which significantly reduces the compressive strength of the sample. At the displacement of 50 mm, rupture has been observed in several transverse reinforcements. After the failure of transverse reinforcements, the structure's performance of columns is severely reduced. As the loading continues, large deformations occur in the circular specimens, and the longitudinal rebars become strongly arched, and in most specimens, due to the creation of the shear surface, the halving mode is observed according to Figs. 8 and 9.

#### 3.3 Comparison of square specimens

Fig. 10 shows the force-displacement curves of all square-section columns. It is clear from Fig. 10 that the highest load-bearing capacity is shown by the specimen S-B containing ECC and U shape curved elements to connect. This specimen achieved a maximum resistance of 434.19 KN, which is 3.23 times greater than the maximum resistance values of the simple specimens S-O without retrofitting. The S-B specimen also showed 8664 KN-mm energy absorption,

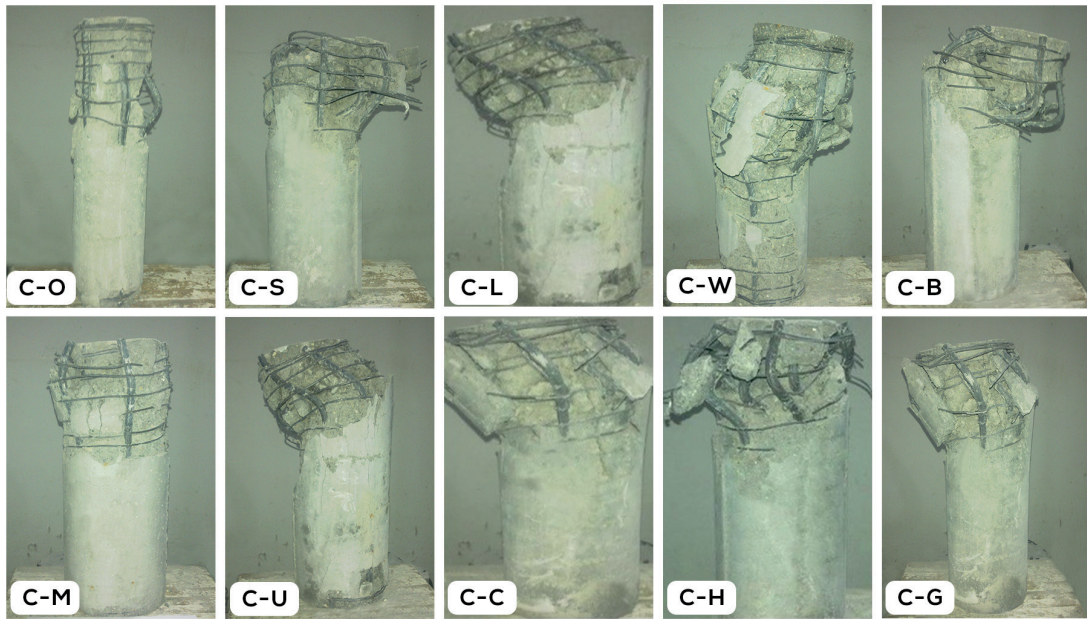


Fig. 8 Damaged form of circle specimens under compression test

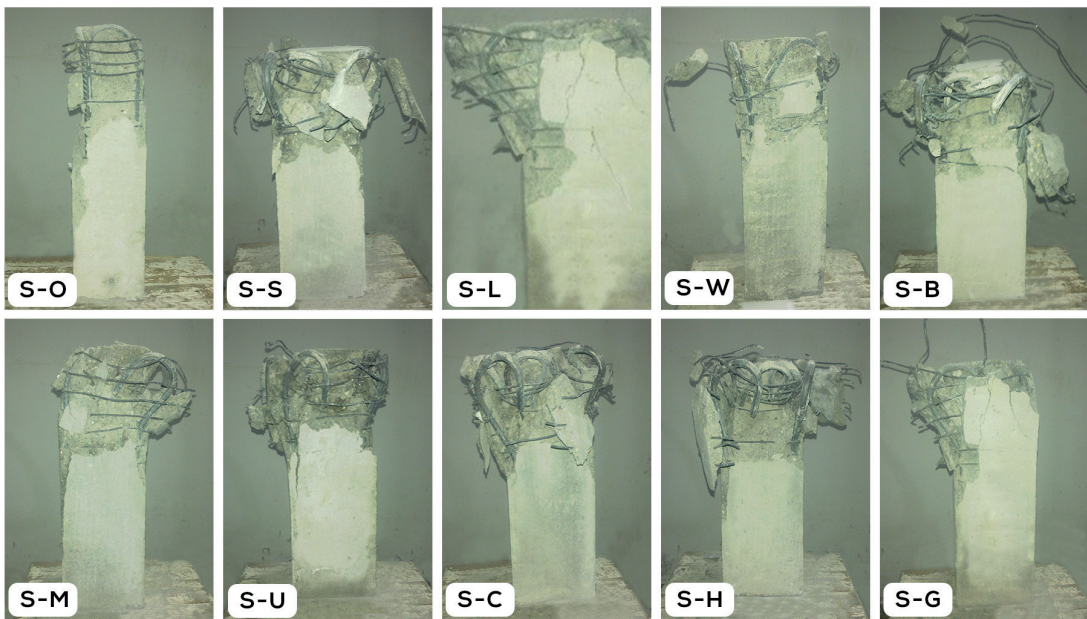


Fig. 9 Damaged form of square specimens under compression test

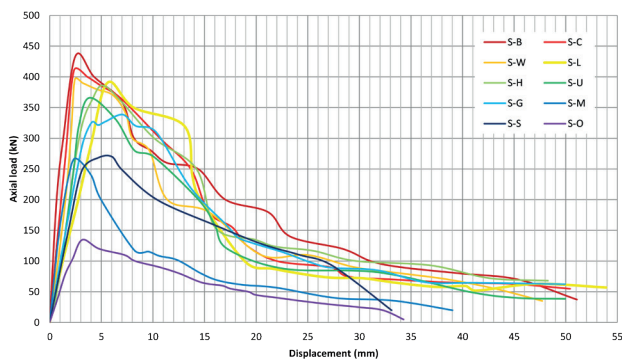


Fig. 10 Force-displacement curves for square specimens

4.14 times more than the simple specimens. With removing the concrete cover of the primary column, the specimen S-C also reached a resistance of 410.45 KN, which is 3.05 times more than the value of the unjacketed columns (S-O). It has the best (maximum) energy absorption of 9064 KN-mm compared to other methods, which is 4.33 more than the energy absorption of primary columns (S-O).

Table 4 was regulated according to the maximum failure force recorded during the testing of specimens (S-B) with 434.19 KN to a minimum value of failure force of specimens (S-O) with 134.57 KN. Additionally, it presents the

percentage of increase in maximum failure force of various jacketed specimens to maximum failure force of unjacketed column specimens. The most significant increase is shown by specimens S-B and C-B of 3.23 and 3.39 belonging to square and circular jacketed columns using ECC of U-shaped elements on the contact surface and removing concrete cover method, respectively. The lowest percentage increases are related to the square and circular unjacketed specimens (S-O and C-O) with a value of 1.0.

Other effective methods include removing the concrete cover of the primary column (S-C) and using galvanized mesh (S-W). The two NC methods, including simple jacketing (S-S) and integrated specimen (S-M), have the lowest strength increases.

### 3.4 Comparison of circular samples

Fig. 11 shows the force-displacement curves of all circular specimens. It is clear from Fig. 11 that the highest load-bearing capacity is shown by specimen C-B containing U-shaped elements using ECC. This specimen achieved a maximum resistance of 560.45 KN, which is 3.39 times greater than the maximum resistance values of the simple primary (unjacketed) specimen. This specimen

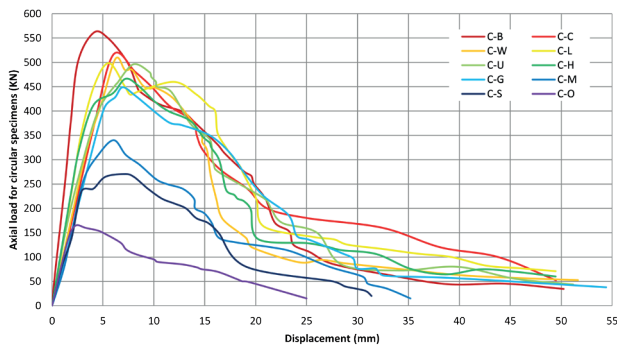


Fig. 11 Force-displacement curves for circular specimens

showed 4.68 times more energy than the unjacketed specimen in terms of energy absorption.

The specimen with simple jacketing using NC (specimen C-S) also achieved a resistance of 270.45 KN, 1.64 times more than the value of the unjacketed specimen (C-O), and it has the weakest performance compared to other methods. In terms of energy absorption, it shows 2.00 times more energy than the specimen C-O. The lowest percentage strength increases among jacketed specimens using ECC is related to the simple jacketing (specimen C-G), but it achieved integrated bearing capacity (C-M).

For favorable comparison, Fig. 12 shows only three specimens, including the using ECC beside U shape elements to connect (C-B), integrated specimen using NC (C-M) and also an unjacketed specimen (C-O). The use of ECC in the jacketing area and U shape elements on the contact surface makes the bearing capacity of the primary column considerably more than the integrated specimen and unjacketed specimen O as well. As it can be seen, the high ductility and maximum failure load of specimens show that using ECC and also suitable connections are remarkably effective techniques.

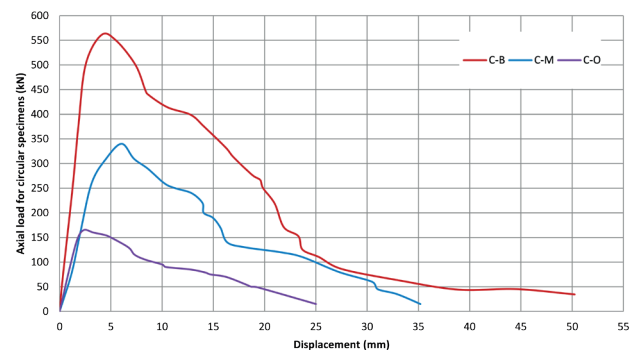


Fig. 12 Force-displacement curve of primary, integrated, and jacketed specimens

Table 4 Experimental results of specimens

Specimen Name	Number of Specimens	Maximum Force (KN)		$P_{retrofit}/P_o$		Energy absorption (KN-mm)		$E_{retrofit}/E_o$	
		S	C	S	C	S	C	S	C
Specimen B	2	434.19	560.45	3.23	3.39	8664	10215	4.14	4.68
Specimen C	2	410.45	515.49	3.05	3.12	9064	10910	4.33	4.99
Specimen W	2	395.85	507.85	2.94	3.07	7034	8794	3.36	4.02
Specimen L	2	390.40	498.56	2.90	3.02	7105	10860	3.39	4.97
Specimen U	2	385.95	495.86	2.87	3.00	7696	9828	3.68	4.50
Specimen H	2	345.80	466.55	2.57	2.82	7351	9517	3.51	4.36
Specimen G	2	338.49	448.95	2.52	2.72	7107	9355	3.40	4.28
Specimen M	2	267.18	340.15	1.99	2.06	4550	5492	2.17	2.51
Specimen S	2	215.22	270.45	1.60	1.64	3456	4373	1.65	2.00
Specimen O*	6	134.57	165.25	1.00	1.00	2093	2185	1.00	1.00

\* The values have been calculated based on the average of the maximum failure load of O-1, O-2, O-3 specimens.

### 3.5 Ductility and energy absorption

Structural elements with high ductility withstand larger inelastic deformations before failure and show a greater ability to absorb energy. As shown in Fig. 13, the specimens with ECC jacketing exhibited significant ductility and energy absorption compared to the ductility and energy absorption of specimens using NC. For instance, a square cross-section specimen with u-shaped elements to connect using ECC (S-B) obtained 8664 KN-mm energy absorption with more than 50 mm displacement at failure point while the specimen using NC jacketing (S-S) had just 3456 KN-mm energy absorption with only 33 mm displacement at the failure point. From Figs. 10 and 11, it is clear that using ECC within the jacketing area leads to higher energy absorption and a more significant displacement during the test and failure point.

### 4 Numerical simulation

Abaqus finite element software was used in the next step to use to model and verify experimental specimens. Then by altering the various input parameters (independent variables), it was aimed to expand models and target variables. Since damage plays the main role in this study, therefore concrete damage plasticity (CDP) has been used to model the plastic behavior of concrete, according to Michal and Andrzej model [33]. The modulus of elasticity and the poisson ratio of concrete and steel are considered 28Gpa, 0.2 and 210 Gpa, and 0.3, respectively. Solid elements (C3D8R) and wire elements (B31) have been used for rebars to model concrete. The two best types of jacketing regarding the experimental test results, Specimen B and Specimen C, have been used to verify and expand numerical models by altering parameters. Table 5 indicates the parameters in FEA models. Fig. 14 illustrates the square and circular column modeled in Abaqus.

All models were subjected to compression tests in a displacement-control analysis. The displacement increases gradually and starts from zero in a linear pattern until it reaches 5 mm at the end of the analysis in the dynamic/explicit step. The reaction force of the end side of the column has been derived, and Load-displacement curves are as below in Fig. 15.

#### 4.1 List of models

Since the numerical and laboratory modeling results are consistent, the models are expanded by changing the parameters. According to Table 6, by changing the parameters of the U-shape element's diameter and the ECC's

strength, the effect of these parameters is discussed to determine which models have the best performance in the two selected optimal types.

### 4.2 Results of simulation

Results indicate that the stress distribution is uniform in circular columns, and both horizontal and vertical rebars share stress tolerance. However, this uniform distribution is not observed in square columns, and most of the

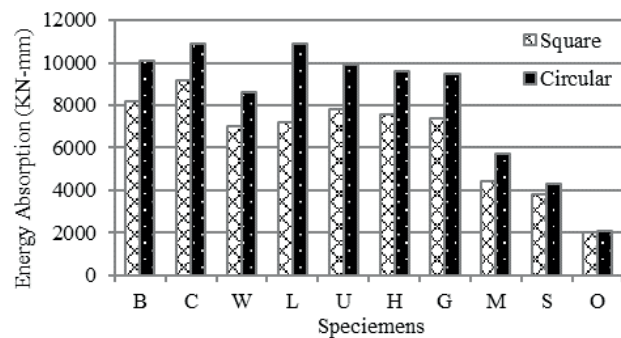


Fig. 13 Comparison of energy absorption of square and circular specimens

Table 5 Material parameters used in the FEA model

Concrete				
Density (kg/m <sup>3</sup> )	Elasticity (GPa)	Poisson's Ratio	$f_c$ (MPa)*	$f_t$ (MPa)
2450	28	0.2	30	3.5
CDP Parameters [33]				
Dilation Angle	Eccentricity	$fb_0/fc_0$	$K$	Viscosity Parameter
30	0.1	1.16	0.667	0.001
Steel				
Density (kg/m <sup>3</sup> )	Elasticity (GPa)	Poisson's Ratio	Yield Strength (MPa)	Yield strain
7850	210	0.3	430	0.00324

\*Compressive strength varies from 30-55 MPa in numerical models and for ECC it is equal to 55 MPa.

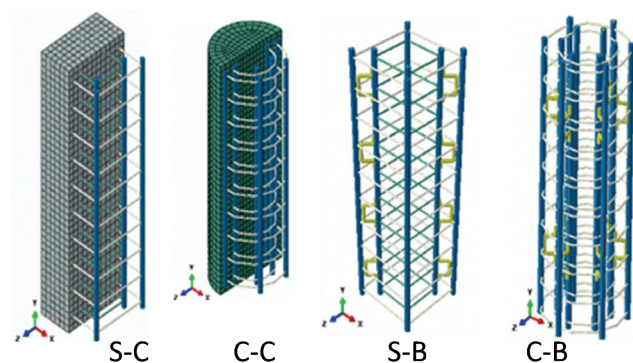


Fig. 14 Abaqus model of square and circular columns

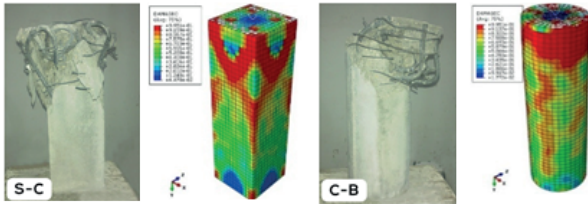
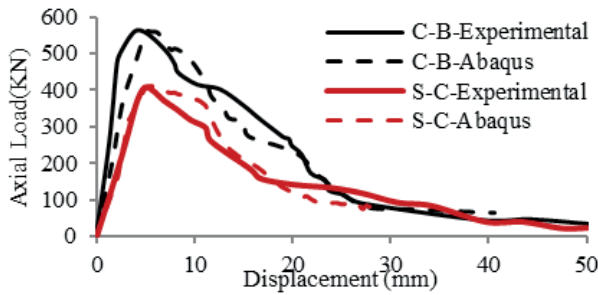


Fig. 15 Comparison of numerical and experimental modeling

Table 6 List of numerical models

Vertical U-Shaped Element Models			Replacing concrete cover by ECC		
Square	Circular	Diameter (mm)	Square	Circular	Compressive strength (Mpa)
S-B	C-B	5	S-C	C-C	40
S-B1	C-B1	10	S-C1	C-C1	55
S-B2	C-B1	8	S-C2	C-C1	50
S-B3	C-B1	6	S-C3	C-C1	45
S-B4	C-B1	4	S-C4	C-C1	35
S-B5	C-B1	3	S-C5	C-C1	30

stresses are borne by vertical rebars and U-shaped joints. In modeling performed by changing the diameter of the U-shaped element, the effect of the diameter of this element on the cohesion of the casing and the core is discussed. This change is done in both circular and square columns. The stress contour created in models S-B and C-B can be seen in Fig. 16. As it illustrates, the stress is in the vertical rebars close to the area under maximum pressure. It is also observed that U-shaped elements withstand stress close to the yield stress, indicating that damage may also occur in these areas. Therefore, by changing the diameter, the stress in these points can be reduced.

The result of compressive loading in Abaqus is shown in Fig. 17. The maximum compressive strength is derived from results and compared to other models.

As it is clear from the results, increasing the ECC strength directly affects the compressive strength of the jacketed column. This effect is such that in a circular column, the use of ECC with a strength of 55 MPa increases

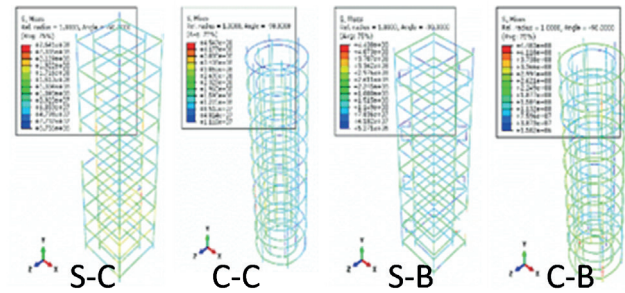


Fig. 16 Stress distribution in reinforcement

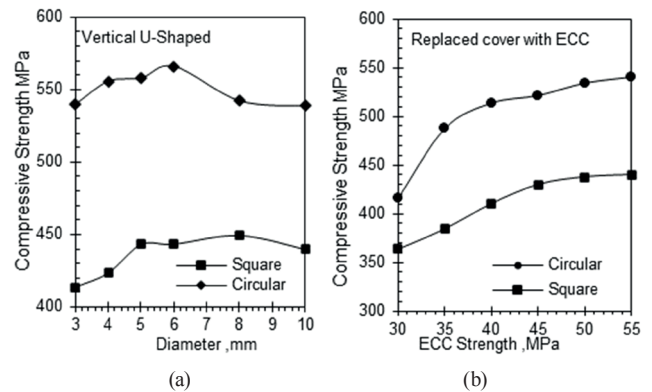


Fig. 17 result of parametric modeling of jacket columns with; a) Vertical U-Shaped elements and b) Replaced cover

the compressive strength of the column by more than 40% compared to an ECC with a strength of 30 MPa. This ratio is lower for square columns and is almost 30%. Results also indicate that in the numerical models, increasing the rebar diameter may even reduce the compressive strength of the column. This is because by increasing the diameter of the u-shaped element, discontinuities may occur in the concrete of the column.

### 5 Conclusions

This study focused on investigating the effectiveness of jacketing square or circular columns with ECC and NC, and different types of connections between the casing and the core. The results obtained from the experiments were compared from different aspects such as ductility, the percentage increase in the initial strength of the columns, and the energy absorption. Additionally, to expand the models, numerical simulations by FEM used, and the effect of U-shaped element's diameter and the compressive strength of ECC were evaluated and compared with experimental models that the following results can be addressed:

1. Concrete jacketing can be improved the bearing capacity of RC columns, especially when using ECC in the jacketing areas.

2. Jacketing of the core in RC columns increases the strength by 1.6 to 3.23 times for square sections, which is by 1.64 to 3.39 times for circular sections.
3. Using ECC as a jacketing material significantly increases energy absorption of the columns by 4.33 and 4.99 times for square and circular specimens, respectively.
4. In both square and circular columns, maximum load-bearing capacity is achieved using ECC and horizontal U-shaped curved elements to connect.

Conversely, minimum load-bearing capacity in square and circular columns is achieved using NC without specific measures for concrete jacketing during casting.

5. Circular sections generally showed higher strengthening, energy absorption, and ductility than their square sections under the same conditions.
6. Nonlinear numerical simulations correlated reasonably well with the experimental results, in particular, for the force- displacement curves.

## References

- [1] Dizaji, M. S., Dizaji, F. S., Taghizadeh, E. "Nonlinear Adaptive Simulation of Concrete Gravity Dams using Generalized Prandtl Neural Networks", *International Research Journal of Engineering and Technology (IRJET)*, 5(6), pp. 1990–1994, 2018.
- [2] Wipf, T. J., Klaiber, F. W., Russo, F. M. "Evaluation of seismic retrofit methods for reinforced concrete bridge columns", Iowa State University, Ames, IA, USA, Rep. NCEER-97-0016, 1997.
- [3] Ersoy, U., Tankut, A.T., Suleiman, R. "Behavior of jacketed columns", *ACI Structural Journal*, 90(3), pp. 288–293, 1993.
- [4] Priestley, M. J. N, Seible, F., Calvi, G. M. "Seismic design and retrofit of bridges", John Wiley and Sons, New York, NY, USA, 1996. <https://doi.org/10.1002/9780470172858>
- [5] Cheong, H. K., MacAlevey, N. "Experimental behavior of jacketed reinforced concrete beams", *Journal of Structural Engineering*, 126(6), pp. 692–699, 2000. [https://doi.org/10.1061/\(ASCE\)0733-9445\(2000\)126:6\(692\)](https://doi.org/10.1061/(ASCE)0733-9445(2000)126:6(692))
- [6] Lehman, D. E., Gookin, S. E., Nacamuli, A. M., Moehle, J. P. "Repair of earthquake-damaged bridge columns", *ACI Structural Journal*, 98(2), pp. 233–242, 2001.
- [7] Vandoros, K. G., Dritsos, S. E. "Axial preloading effects when reinforced concrete columns are strengthened by concrete jackets", *Progress in Structural Engineering and Materials*, 8(3), pp. 79–92, 2006. <https://doi.org/10.1002/pse.215>
- [8] Bett, B. J., Klingner, R. E., Jirsa, J. O. "Lateral load response of strengthened and repaired reinforced concrete columns", *Structural Journal*, 85(5), pp. 499–508, 1988.
- [9] Thermou, G. E., Pantazopoulou, S. J., Elnashai, A. S. "Flexural behavior of brittle RC members rehabilitated with concrete jacketing", *Journal of Structural Engineering*, 133(10), pp. 1373–1384, 2007. [https://doi.org/10.1061/\(ASCE\)0733-9445\(2007\)133:10\(1373\)](https://doi.org/10.1061/(ASCE)0733-9445(2007)133:10(1373))
- [10] Ong, K. C. G., Kog, Y. C., Yu, C. H., Sreekanth, A. P.V. "Jacketing of reinforced concrete columns subjected to axial load", *Magazine of Concrete Research*, 56(2), pp. 89–98, 2004. <https://doi.org/10.1680/macr.2004.56.2.89>
- [11] Vandoros, K. G., Dritsos, S. E. "Concrete jacket construction detail effectiveness when strengthening RC columns", *Construction and Building Materials*, 22(3), pp. 264–276, 2008. <https://doi.org/10.1016/j.conbuildmat.2006.08.019>
- [12] Assa, B., Nishiyama, M., Watanabe, F. "New approach for modeling confined concrete. I: Circular Columns", *Journal of Structural Engineering*, 127(7), pp. 743–750, 2001. [https://doi.org/10.1061/\(ASCE\)0733-9445\(2001\)127:7\(743\)](https://doi.org/10.1061/(ASCE)0733-9445(2001)127:7(743))
- [13] Saatcioglu, M., Razvi, S. R. "Strength and ductility of confined concrete", *Journal of Structural Engineering*, 118(6), pp. 1590–1607, 1992. [https://doi.org/10.1061/\(ASCE\)0733-9445\(1992\)118:6\(1590\)](https://doi.org/10.1061/(ASCE)0733-9445(1992)118:6(1590))
- [14] Mander, J. B., Priestley, M. J. N., Park, R. "Observed stress-strain behavior of confined concrete", *Journal of Structural Engineering*, 114(8), pp. 1827–1849, 1988. [https://doi.org/10.1061/\(ASCE\)0733-9445\(1988\)114:8\(1827\)](https://doi.org/10.1061/(ASCE)0733-9445(1988)114:8(1827))
- [15] Mander, J. B., Priestley, M. J. N., Park, R. "Theoretical stress-strain model for confined concrete", *Journal of Structural Engineering*, 114(8), pp. 1804–1826, 1988. [https://doi.org/10.1061/\(ASCE\)0733-9445\(1988\)114:8\(1804\)](https://doi.org/10.1061/(ASCE)0733-9445(1988)114:8(1804))
- [16] Hoshikuma, J., Kawashima, K., Nagaya, K., Taylor, A. W. "Stress-strain model for confined reinforced concrete in bridge piers", *Journal of Structural Engineering*, 123(5), pp. 624–633, 1997. [https://doi.org/10.1061/\(ASCE\)0733-9445\(1997\)123:5\(624\)](https://doi.org/10.1061/(ASCE)0733-9445(1997)123:5(624))
- [17] Pourbaba, M., Asefi, E., Sadaghian, H., Mirmiran, A. "Effect of age on the compressive strength of ultra-high-performance fiber-reinforced concrete", *Construction and Building Materials*, 175, pp. 402–410, 2018. <https://doi.org/10.1016/j.conbuildmat.2018.04.203>
- [18] Pourbaba, M., Joghataie, A., Mirmiran, A. "Shear behavior of ultra-high performance concrete", *Construction and Building Materials*, 183, pp. 554–564, 2018. <https://doi.org/10.1016/j.conbuildmat.2018.06.117>
- [19] Ahangarnazhad, B. H., Pourbaba, M., Afkar, A. "Bond behavior between steel and Glass Fiber Reinforced Polymer (GFRP) bars and ultra-high performance concrete reinforced by Multi-Walled Carbon Nanotube (MWCNT)", *Steel and Composite Structures*, 35(4), pp. 463–474, 2020. <http://dx.doi.org/10.12989/scs.2020.35.4.463>
- [20] Dadmand, B., Pourbaba, M., Sadaghian, H., Mirmiran, A. "Experimental & numerical investigation of mechanical properties in steel fiber-reinforced UHPC", *Computers and Concrete*, 26(5), pp. 451–465, 2020. <http://dx.doi.org/10.12989/cac.2020.26.5.451>

- [21] Dadmand, B., Pourbaba, M., Sadaghian, H., Mirmiran, A. "Effectiveness of steel fibers in ultra-high-performance fiber-reinforced concrete construction", *Advances in Concrete Construction*, 10(3), pp. 195–209, 2020.  
<https://doi.org/10.12989/acc.2020.10.3.195>
- [22] Pourbaba, M., Sadaghian, H., Mirmiran, A. "Flexural response of UHPFRC beams reinforced with steel rebars", *Advances in Civil Engineering Materials*, 8(3), pp. 411–430, 2019.  
<https://doi.org/10.1520/ACEM20190129>
- [23] Pourbaba, M., Sadaghian, H., Mirmiran, A. "A comparative study of flexural and shear behavior of ultra-high-performance fiber-reinforced concrete beams", *Advances in Structural Engineering*, 22(7), pp. 1727–1738, 2019.  
<https://doi.org/10.1177/1369433218823848>
- [24] Pourbaba, M., Joghataie, A. "Determining shear capacity of ultra-high performance concrete beams by experiments and comparison with codes", *Scientia Iranica*, 26(1), pp. 273–282, 2019.  
<https://doi.org/10.24200/SCI.2017.4264>
- [25] Li, V. C. "On engineered cementitious composites (ECC)", *Journal of Advanced Concrete Technology*, 1(3), pp. 215–230, 2003.
- [26] Li, V. C., Horii, H., Kabele, P., Kanda, T., Lim, Y. M. "Repair and retrofit with engineered cementitious composites", *Engineering Fracture Mechanics*, 65(2–3), pp. 317–334, 2000.
- [27] Li, V. C. "Engineered Cementitious Composites (ECC) - Bendable Concrete for Sustainable and Resilient Infrastructure", Springer, Berlin, Heidelberg, Germany, 2019.  
<https://doi.org/10.1007/978-3-662-58438-5>
- [28] Li, V. C., Wang, S., Wu, C. "Tensile strain-hardening behavior of polyvinyl alcohol engineered cementitious composite (PVA-ECC)", *ACI Materials Journal*, 98(6), pp. 483–492, 2001.
- [29] Krishnaraja, A. R., Kandasamy, S. "Flexural performance of hybrid engineered cementitious composite layered reinforced concrete beams", *Periodica Polytechnica Civil Engineering*, 62(4), pp. 921–929, 2018.  
<https://doi.org/10.3311/PPci.11748>
- [30] ASTM "ASTM C150/C150M-17 Standard Specification for Portland Cement", ASTM International, West Conshohocken, PA, USA, 2017.  
[https://doi.org/10.1520/C0150\\_C0150M-17](https://doi.org/10.1520/C0150_C0150M-17)
- [31] ASTM "ASTM C618-19 Standard Specification for Coal Fly Ash and Raw or Calcined Natural Pozzolan for use as a Mineral Admixture in Concrete", ASTM International, West Conshohocken, PA, USA, 1997.  
<https://doi.org/10.1520/C0618-19>
- [32] ASTM "ASTM C494M-17 Standard Specification for Chemical Admixtures for Concrete", ASTM International, ASTM International, West Conshohocken, PA, USA, 2017.  
[https://doi.org/10.1520/C0494\\_C0494M-19](https://doi.org/10.1520/C0494_C0494M-19)
- [33] Michał, S., Andrzej, W. "Calibration of the CDP model parameters in Abaqus", presented at The 2015 World Congress on Advances in Structural Engineering and Mechanics (ASEM15), Incheon, Korea, Aug. 25–29, 2015.